Preprints of the 19th World Congress
The International Federation of Automatic Control
Cape Town, South Africa. August 24-29, 2014

Digital Control of a Camless Engine Using Lyapunov Approach with Backward Euler Approximation ⋆

Paolo Mercorelli * **Nils Werner Udo Becker** **
Horst Harndorf *** **Theo van Niekerk** ****

* *Institute of Product and Process Innovation*
Leuphana University of Lueneburg
Volgershall 1, D-21339 Lueneburg, Germany
(e-mail: mercorelli@uni.leuphana.de)
** *Faculty of Automotive Engineering*
Ostfalia University of Applied Sciences
Kleiststr. 14-16, D-38440 Wolfsburg, Germany
(e-mails: n.werner@ostfalia.de, u.becker@ostfalia.de)
*** *Fakultät für Maschinenbau und Schiffstechnik*
Universität Rostock
Albert-Einstein-Str., D-218059 Rostock, Germany
(e-mail: horst.harndorf@uni-rostock.de)
**** *Department of Mechatronics*
Nelson Mandela Metropolitan University
Port Elizabeth, 6031, South Africa
(e-mail: theo.vanNiekerk@nmmu.ac.za)

Abstract:
In this paper a modelling of a hybrid actuator is proposed. The hybrid actuator consists of a piezo, a mechanical and a hydraulic ratio displacement. This paper deals with a hybrid actuator composed by a piezo, and a hydraulic part controlled using a regulator for camless engine motor applications. The discrete control law is derived using the well-known Backward Euler method. An analysis of the Backward and Forward Euler method is also presented. Simulations with real data are shown.

Keywords: Actuators, Digital control, Lyapunov methods, Engine control.

1. INTRODUCTION

In the variegated scenario of the possible actuator to be used it is always difficult to be able to choose the best one for a given application. Possible solutions are very often found just considering hybrid actuators as a combination of different ones. Concerning the electromagnetic actuators, there is a new general orientation to use them such as recently described in Mercorelli (2012a). In Mercorelli (2012a) a U-magnet structure is considered in which the Maxwell attracting force is quadratic to the current and inversely quadratic to the distance between the valve armature and the electromagnets. Using the topology presented in Mercorelli (2012a), it is possible to have the availability of a very big force with a small current. Nevertheless, difficulties connected with the control structure and in particular with the control for high cycles of the motor encouraged us to test other topologies. In this phase of the research two kinds of actuators are considered. The first one is a geometric rotational actuator as shown in Mercorelli (2012c), Mercorelli (2012b) and in Fabbrini et al. (2012) in which some fundamental aspects concerning its functionality starting from the optimization of its movement to the control algorithm design are considered. This kind of actuators presents a high value of inductance which can generate some problems of the electromagnetic compatibility with the environment. Moreover, a high value of inductance represents an inertial aspect in the control system. Therefore, innovative and alternative concepts are required to reduce the losses and drawbacks while keeping a high actuator dynamics which are characterized by a high value of velocity and generated force. The idea which this paper presents is to use a hybrid actuator composed by a piezo, a mechanical and a hydraulic part in order to take advantages of all of them. In fact, the piezo electric actuator (PA) has been used in precise positioning applications such as, for instance, atomic force microscopy Croft et al. (2001). The main advantages of PA are nanometer scale, high stiffness, and fast response. However, since PA has nonlinear property which is called hysteresis effect, it leads to inaccuracy in positioning control with a high precise performance. The paper is organised in the following way. In Section 2 an introduction on the general structure of the aggregate actuator is given. Section 3 shows the model of

⋆ This work was financially supported by Bundesministerium für Bildung und Forschung of Germany.

the actuator. After that, in Section 4, the control laws are derived. The paper ends with Section 5 in which simulation results of the proposed valve using real data are presented. After that, the conclusions follow.

2. GENERAL STRUCTURE OF THE AGGREGATE ACTUATOR

In the diagram of Fig. 1 the T-A connection links the couple of valves with the tank and the P-B connection links the couple of valves with the pump. In the position of Fig. 1 connections T-A and P-B are maximally open and the couple of valves are closed because point B is under pressure. When the piezo acts its force, the mechanical servo valve moves and begins to close these connections. When the mechanical servo valve is in the middle position, both connections (T-A and P-B) are closed and connections A-P and B-T begin to open. At this position also both motor valves begin to open because point A is under pressure. Figure 1 shows in detail a part

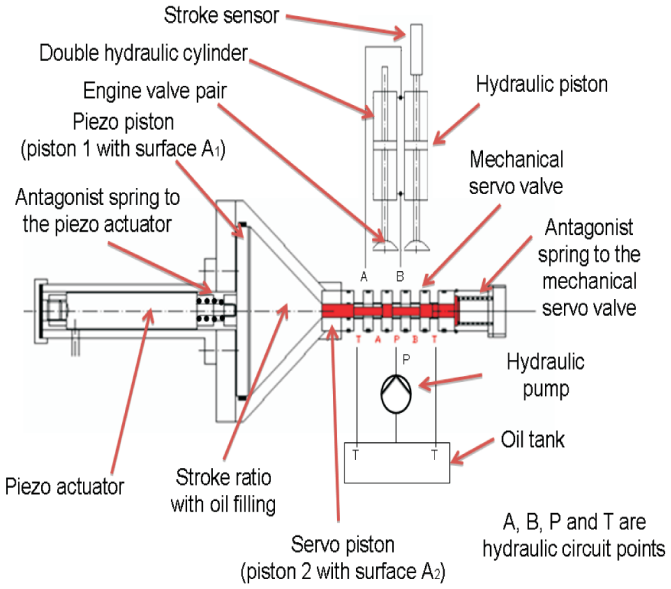

Fig. 1. Scheme of the whole actuator

of the hybrid structure which consists of a piezo actuator combined with a mechanical part. These two parts are connected by a stroke ratio to adapt the stroke length. The proposed nonlinearity model for PEA is quite similar to these presented in Adriaens et al. (2000) and in Yu and Lee (2005) which show a sandwich model for a PEA. Fig. 3 shows the equivalent circuitry for a PEA with the I-layer nonlinearities of hysteresis and creep, in which two I-layers are combined together as C_a and R_a. The I-layer capacitor, C_a, is an ordinary one, which might be varied slightly with some factors, but here it would be assumed constant first for simplicity. The I-layer resistor, R_a , however, is really an extraordinary one with a significant nonlinearity. The resistance is either fairly large, say $R_a > 10^6\ \Omega$, when the voltage $\|V_a\| < V_h$, or is fairly small, say $R_a < 1000$, when $\|V_a\| > V_h$. In Yu and Lee (2005), the threshold voltage, V_h, is defined as the hysteresis voltage of a PEA. The authors in Yu and Lee (2005) gave this definition due to the observation that there is a significant difference and an

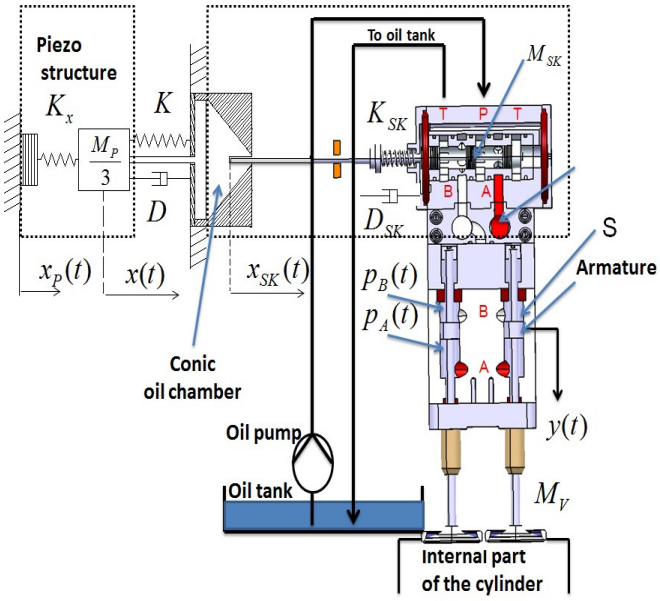

Fig. 2. Detailed scheme of the whole actuator

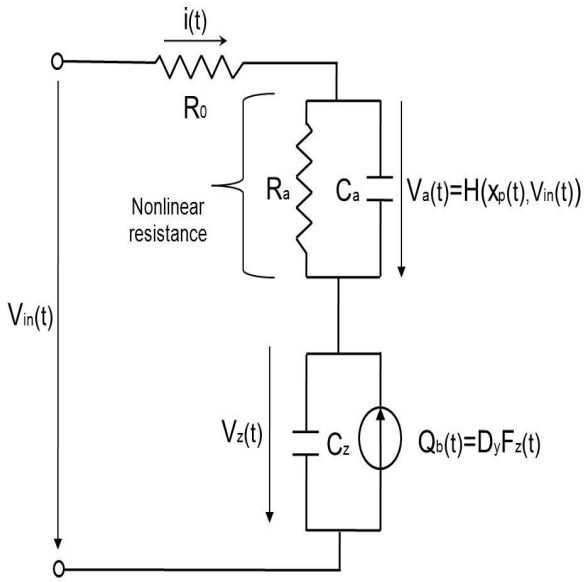

Fig. 3. Electrical part of the model

abrupt change in resistance across this threshold voltage and it is this resistance difference and change across V_h that introduces the nonlinearities of hysteresis and creep in a PEA. The hysteresis effect could be seen as a function of input $V_{in}(t)$ and output $y(t)$ as follows: $H(y(t), V_{in}(t))$. According to this model, if $V_h = 0$, then the hysteresis will disappear, and if $R_a = \infty$ when $\|V_a\| < V_h$, then the creep will also disappear. Based on this proposed sandwich model and the equivalent circuitry as shown in Fig. 3, we can further derive the state model as follows:

$$\dot{V}_a(t) = -\Big(\frac{1}{R_a} + \frac{1}{R_o}\Big)\frac{V_a(t)}{C_a} - \frac{V_z(t)}{C_a R_o} + \frac{V_{in}(t)}{C_a R_o} \quad (1)$$

$$\dot{V}_z(t) = \frac{\dot{Q}_b}{C_z} + \frac{1}{C_z}\Big(-\frac{V_a(t)}{R_o} - \frac{V_z(t)}{R_o} + \frac{V_{in}(t)}{R_o}\Big), \quad (2)$$

where $Q_b = D_y F_z(t)$ is the "back electric charge force" (back-ecf) in a PEA, see Yu and Lee (2005). According to Yu and Lee (2005) and the notation of Fig. 2, it is possible to write:

$$F_z(t) = M_p/3\ddot{x}(t) + D\dot{x}(t) + Kx(t) + K_x x(t). \quad (3)$$

K and D are the elasticity and the friction constant of the spring which is antagonist to the piezo effect and is incorporated in the PEA. C_z is the total capacitance of the PEA and R_o is the contact resistance. For further details on this model see Yu and Lee (2005). Considering the whole system described in Fig. 2 with the assumptions of incompressibility of the oil, the whole mechanical system can be represented by a spring mass structure as shown in the conceptual scheme of Fig. 2. In this system the following notation is adopted: K_x is the elasticity constant factor of the PEA. In the technical literature, factor $D_x K_x = T_{em}$ is known with the name "transformer ratio" and states the most important characteristic of the electromechanical transducer. $M_p/3$ is, in our case, the moving mass of the piezo structure which is a fraction of whole piezo mass, M_{SK} is the sum of the mass of the piston with the oil and the moving actuator and M_v is the mass of the valve. It is possible to notice that the moving mass of the piezo structure is just a fraction of the whole piezo mass. The value of this fraction is given by the constructer of the piezo device and it is determined by experimental measurements. K_{SK} and D_{SK} are the characteristics of the antagonist spring to the mechanical servo valve, see Fig. 2. D_{oil} is the friction constant of the oil. Moreover, according to Yu and Lee (2005), motion $x_p(t)$ is:

$$x_p(t) = D_x V_z(t). \quad (4)$$

According to the diagram of Fig. 3, it is possible to write as follows:

$$V_z = V_{in}(t) - R_0 i(t) - H(x_p(t), V_{in}(t)), \quad (5)$$

where R_0 is the connection resistance and $i(t)$ is the input current as shown in Fig. 3.

3. MODEL OF THE HYBRID ACTUATOR

For a piezo actuator, in the technical literature, factor $D_x K_x = T_{em}$ is known with the name "transformer ratio" and states the most important characteristic of the electromechanical transducer in which K_x is the elasticity constant factor of the PEA and D_x is the parameter which is responsible to transform voltage into movement. In fact, another well-known physical relation is $= F_1 = D_x K_x V_z$ which represents the piezo force in which V_z is the internal voltage. In the ideal case we have that $V_z = V_{in}$ where V_{in} states the input voltage. If the model in Fig. 4 is considered, then:

$$M_P \cdot \ddot{x}_1(t) = V_z(t) D_x K_x - K_{FL1} \cdot (x_1(t) - x_c(t)) - (K_x + K) \cdot x_1(t) - D\dot{x}_1(t), \quad (6)$$

together with

$$0 = 0 - K_{FL1} \cdot (x_c(t) - x_1(t)) - K_{FL2} \cdot (x_c(t) - x_2(t)), \quad (7)$$

and

$$M_{SK} \cdot \ddot{x}_2(t) = 0 - K_{FL2} \cdot (x_2(t) - x_c(t)) - K_{SK} \cdot x_2(t) - D_{SK} \cdot \dot{x}_2(t). \quad (8)$$

Considering Eq. (7) the following expression is obtained:

$$x_c(t) = \frac{K_{FL1} \cdot x_1(t) + K_{FL2} \cdot x_2(t)}{K_{FL1} + K_{FL2}}, \quad (9)$$

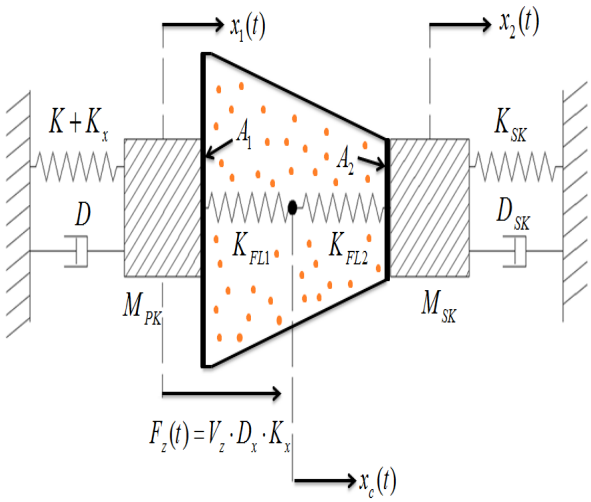

Fig. 4. Model of the piezo mechanical part of the actuator

and substituting Eq. (9) into Eq. (8) the following expression is obtained:

$$M_{SK} \cdot \ddot{x}_2(t) = -K_{FL2} \cdot x_2(t) - K_{SK} \cdot x_2(t) - D_{SK} \cdot \dot{x}_2(t) + K_{FL2} \cdot \frac{K_{FL1} \cdot x_1(t) + K_{FL2} \cdot x_2(t)}{K_{FL1} + K_{FL2}}. \quad (10)$$

With the help of Laplace transformation it is obtained that:

$$s^2 M_{SK} \cdot X_2(s) = -K_{FL2} \cdot X_2(s) - K_{SK} \cdot X_2(s) - sD_{SK} \cdot X_2(s) + \frac{K_{FL1} \cdot K_{FL2} \cdot X_1(s) + K_{FL2}^2 \cdot X_2(s)}{K_{FL1} + K_{FL2}}, \quad (11)$$

$$s^2 M_{SK} \cdot (K_{FL1} + K_{FL2}) \cdot X_2(s) = -K_{FL1} \cdot K_{FL2} \cdot X_2(s) - K_{FL2}^2 \cdot X_2(s) - K_{SK} \cdot (K_{FL1} + K_{FL2}) \cdot X_2(s) - s \cdot D_{SK} \cdot (K_{FL1} + K_{FL2}) \cdot X_2(s) + K_{FL1} \cdot K_{FL2} \cdot X_1(s) + K_{FL2}^2 \cdot X_2(s), \quad (12)$$

$$X_2(s) \cdot (s^2 M_{SK} \cdot (K_{FL1} + K_{FL2}) + s \cdot D_{SK} \cdot (K_{FL1} + K_{FL2}) + (K_{FL1} \cdot K_{FL2} + K_{SK} \cdot (K_{FL1} + K_{FL2})) = X_1(s) \cdot K_{FL1} \cdot K_{FL2}, \quad (13)$$

and

$$\frac{X_2(s)}{X_1(s)} = \frac{K_{FL1} \cdot K_{FL2}}{(s^2 M_{SK} + s \cdot D_{SK} + K_{SK}) \cdot (K_{FL1} + K_{FL2}) + K_{FL1} \cdot K_{FL2}} \quad (14)$$

and thus:

$$\frac{X_2(s)}{X_1(s)} = \frac{\frac{K_{FL1} \cdot K_{FL2}}{K_{FL1} + K_{FL2}}}{s^2 M_{SK} + s \cdot D_{SK} + K_{SK} + \frac{K_{FL1} \cdot K_{FL2}}{K_{FL1} + K_{FL2}}}. \quad (15)$$

Considering A_1 and A_2 of the hydraulic position ratio with the two hydraulic springs:

$$\frac{X_2(s)}{X_1(s)} = \frac{A_1}{A_2} \cdot \frac{\frac{K_{FL1} \cdot K_{FL2}}{K_{FL1} + K_{FL2}}}{s^2 M_{SK} + s \cdot D_{SK} + K_{SK} + \frac{K_{FL1} \cdot K_{FL2}}{K_{FL1} + K_{FL2}}}, \quad (16)$$

with the help of Eq. (6) the following expression is obtained:

$$s^2 \cdot M_P \cdot X_1(s) = V_z(s) D_x K_x - K_{FL1} \cdot (X_1(s) - X_c(s)) - (K_x + K) \cdot X_1(s) - s \cdot D \cdot X_1(s), \quad (17)$$

and from (9) it follows that:

$$X_c(s) = \frac{K_{FL1} \cdot X_1(s) + K_{FL2} \cdot X_2(s)}{K_{FL1} + K_{FL2}}. \quad (18)$$

Using (18) together with (17) the following final expression is obtained:

$$s^2 \cdot M_P \cdot X_1(s) = V_z(s) D_x K_x - K_{FL1} \cdot (X_1(s) - \frac{K_{FL1} \cdot X_1(s) + K_{FL2} \cdot X_2(s)}{K_{FL1} + K_{FL2}}) - (K_x + K) \cdot X_1(s) - s \cdot D \cdot X_1(s). \quad (19)$$

In the range of frequency between 0 and 60 Hz the transfer function of such an actuator can be considered, in the first approximation, as a constant. From Eq. 19 the following expression is obtained:

$$s^2 \cdot M_P \cdot X_1(s) = V_z(s) D_x K_x - K_{FL1} \cdot X_1(s) + \frac{K_{FL1}^2}{K_{FL1} + K_{FL2}} \cdot X_1(s) + b_1 \cdot X_2(s) - (K_x + K) \cdot X_1(s) - s \cdot D \cdot X_1(s), \quad (20)$$

where:

$$b_1 = \frac{K_{FL1} \cdot K_{FL2}}{K_{FL1} + K_{FL2}}, \quad (21)$$

and the following expression is derived:

$$\frac{X_1(s)}{V_z(s) D_x K x + b_1 \cdot X_2(s)} = \frac{1}{M_P \cdot s^2 + D \cdot s + K_{FL1} + K_x + K - \frac{K_{FL1}^2}{K_{FL1} + K_{FL2}}}. \quad (22)$$

Using Eq. (16) the final transfer function is obtained:

$$X_2(s) = \frac{A_1}{A_2} \cdot \frac{b_1}{M_{SK} \cdot s^2 + D_{SK} \cdot s + K_{SK} + b_1} \cdot X_1(s). \quad (23)$$

Combining Eqs. (22) with (23), the following expression is obtained:

$$\frac{X_2(s)}{F_z(s)} = \frac{\Omega_0}{\Omega_4 s^4 + \Omega_3 s^3 + \Omega_2 s^2 + \Omega_1 s + 1}, \quad (24)$$

where:

$$\Omega_0 = \frac{1}{K_{01} K_{04} - b_1}, \quad (25)$$

$$\Omega_4 = \frac{K_{03} M_{PK}}{K_{01} K_{04} - b_1}, \quad (26)$$

$$\Omega_3 = \frac{(K_{03} D + K_{02} M_{PK})}{K_{01} K_{04} - b_1}, \quad (27)$$

$$\Omega_2 = \frac{K_{05}}{K_{01} K_{04} - b_1}, \quad (28)$$

and

$$\Omega_1 = \frac{(K_{02} K_{04} + K_{01} D)}{K_{01} K_{04} - b_1}, \quad (29)$$

with

$$K_{01} = \frac{A_2 \cdot K_{SK} + A_2 \cdot b_1}{A_1 \cdot b_1}, \quad (30)$$

$$K_{02} = \frac{A_2}{A_1 \cdot b_1} \cdot D_{SK}, \quad (31)$$

$$K_{03} = \frac{A_2}{A_1 \cdot b_1} \cdot M_{SK}, \quad (32)$$

$$K_{04} = K_{FL1} + K_x + K - \frac{K_{FL1}^2}{K_{FL1} + K_{FL2}}, \quad (33)$$

$$K_{05} = K_{03} K_{04} + K_{02} D + K_{01} M_{PK}. \quad (34)$$

3.1 Hydraulic part of the actuator

In Fig. 5 a possible linear model which is often utilised in practical applications is presented. The model was presented in Murrenhoff (2002) and it is a possible linear approximation utilized in many industrial applications, see industrial cases presented in Murrenhoff (2002). In Fig. 5 this model in which, the following parameters are visible, is represented: T_H which represents the time constant of the hydraulic part, T_M which represents the time constant of the mechanic part. V_H and V_M represent the steady state factors of the hydraulic and mechanical transfer function respectively. The other parameter which characterises the hydraulic-mechanical model is $K2Lidx$. In fact, parameter $K2Lidx$ is a characteristic value of the velocity-dependent internal leakage. This parameter multiplied by the velocity of the valve states a loosing mass flux as represented in the block diagram of Fig. 5. Parameter A_{AK} is the surface of the moving part (servo piston). Observing Fig. 5 and

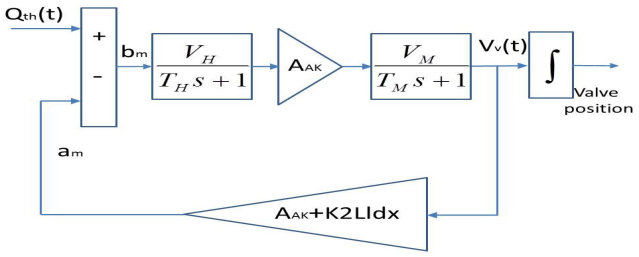

Fig. 5. Hydraulic model structure

considering that variable Q_{th} is the mass flux involved in the hydraulic actuator, the following calculations are derived:

$$b_m = Q_{th}(s) - a_m, \quad (35)$$

$$V_V(s) = b_m \cdot \frac{V_H \cdot V_M \cdot A_{AK}}{(T_H \cdot s + 1) \cdot (T_M \cdot s + 1)}, \quad (36)$$

$$V_V(s) = b_m \cdot \frac{V_H \cdot V_M \cdot A_{AK}}{T_H \cdot T_M \cdot s^2 + (T_H + T_M) \cdot s + 1} \quad (37)$$

$$a_m = V_V(s) \cdot (A_{AK} + K2Lidx), \quad (38)$$

$$b_m = Q_{th}(s) - V_V(s) \cdot (A_{AK} + K2Lidx), \quad (39)$$

$$V_V(s) = (Q_{th}(s) - V_V(s) \cdot (A_{AK} + K2Lidx)) \cdot \frac{V_H \cdot V_M \cdot A_{AK}}{T_H \cdot T_M \cdot s^2 + (T_H + T_M) \cdot s + 1}. \quad (40)$$

Considering the transfer function, then:

$$\frac{V_V(s)}{Q_{th}(s)} = \frac{d_m}{a_m \cdot s^2 + b_m \cdot s + c_m}, \quad (41)$$

where:

$$a_m = T_H \cdot T_M, \quad (42)$$

$$b_m = (T_H + T_M), \tag{43}$$
$$c_m = 1 + V_H \cdot V_M \cdot A_{AK} \cdot (A_{AK} + K2Lidx), \tag{44}$$
$$d_m = V_H \cdot V_M \cdot A_{AK}, \tag{45}$$
$$a_m \cdot s^2 \cdot V_V(s) + b_m \cdot s \cdot V_V(s) + c_m \cdot V_V(s) - d_m \cdot Q_{th}(s) = 0. \tag{46}$$

Considering the Back Laplace transform, then:

$$a_m \cdot \ddot{V}_V(t) + b_m \cdot \dot{V}_V(t) + c_m \cdot V_V(t) - d_m \cdot Q_{th}(t) = 0. \tag{47}$$

If the following positions are considered:

$$x_1(t) = V_V(t), \tag{48}$$
$$x_2(t) = \dot{x}_1(t), \tag{49}$$

then:

$$\dot{x}_1(t) = x_2(t), \tag{50}$$
$$\dot{x}_2(t) = \frac{1}{a_m} \cdot (d_m \cdot Q_{th}(t) - b_m \cdot x_2(t) - c_m \cdot x_1(t)), \tag{51}$$

and

$$\begin{bmatrix} \dot{x}_1(t) \\ \dot{x}_2(t) \end{bmatrix} = \begin{bmatrix} 0 & 1 \\ -\frac{c_m}{a_m} & -\frac{b_m}{a_m} \end{bmatrix} \cdot \begin{bmatrix} x_1(t) \\ x_2(t) \end{bmatrix} + \begin{bmatrix} 0 \\ \frac{d_m}{a_m} \end{bmatrix} \cdot Q_{th}(t). \tag{52}$$

It is possible to write the following general equation:

$$\dot{\mathbf{x}}(t) = \mathbf{A}_m \cdot \mathbf{x}(t) + \mathbf{B}_m \cdot Q_{th}(t). \tag{53}$$

4. CONTROL SYSTEM

Figure 6 shows the control system structure which consists of an inversion of the piezo mechanical system together with a Lyapunov based controller. This inversion is a standard one and for sake of brevity just the Lyapunov controller will be considered. The following sliding function is defined:

$$s(t) = \mathbf{G}\big(\mathbf{x}_d(t) - \mathbf{x}(t)\big), \tag{54}$$

where $\mathbf{G} = [\,\lambda\ 1\,]$, and $\mathbf{x}_d(t)$ represents the vector of the desired trajectories. Equation (54) becomes as follows:

$$s(t) = [\,\lambda\ 1\,] \begin{bmatrix} x_{1d}(t) - x_1(t) \\ x_{2d}(t) - x_2(t) \end{bmatrix}, \tag{55}$$

thus:

$$s(t) = \lambda\big(x_{1d}(t) - x_1(t)\big) + x_{2d}(t) - x_2(t). \tag{56}$$

If the following Lyapunov function is defined:

$$V(s) = \frac{s^2(t)}{2}, \tag{57}$$

then it follows that:

$$\dot{V}(s) = s(t)\dot{s}(t). \tag{58}$$

In order to find the stability of the solution $s(t) = 0$, it is possible to choose the following function:

$$\dot{V}(s) = -\eta(t)s^2(t), \tag{59}$$

with $\eta > 0$. Comparing (58) with (59), the following relationship is obtained:

$$s(t)\dot{s}(t) = -\eta s^2(t), \tag{60}$$

and finally:

$$s(t)\big(\dot{s}(t) + \eta s(t)\big) = 0. \tag{61}$$

The no-trivial solution follows from the condition

$$\dot{s}(t) + \eta s(t) = 0. \tag{62}$$

From (54) it follows:

$$\dot{s}(t) = \mathbf{G}\big(\dot{\mathbf{x}}_d(t) - \dot{\mathbf{x}}(t)\big) = \mathbf{G}\dot{\mathbf{x}}_d(t) - \mathbf{G}\dot{\mathbf{x}}(t), \tag{63}$$

and thus:

$$\mathbf{G}\big(\dot{\mathbf{x}}_d(t) - \dot{\mathbf{x}}(t)\big) + \mathbf{G}\eta\big(\mathbf{x}_d(t) - \mathbf{x}(t)\big) = 0. \tag{64}$$

If the Backward Euler sampling method is considered for the control law, then from Eqs. (53) and (64) it follows:

$$Q_{th}(k) = -(\mathbf{G}\mathbf{B}_m)^{-1} \cdot \Big(\mathbf{G}\mathbf{A}_m \cdot \mathbf{x}(k) - \mathbf{G}\frac{\mathbf{x}_d(k) - \mathbf{x}_d(k-1)}{T_s} - \eta\mathbf{G}\big(\mathbf{x}_d(k) + \mathbf{x}(k)\big)\Big), \tag{65}$$

where Moore-Penrose Pseudoinverse of $\mathbf{B}_m$ is used. Equation (64) states the following error dynamics:

$$\dot{\mathbf{e}}(t) + \eta\mathbf{e}(t) = 0. \tag{66}$$

Considering the Forward Euler sampling approximation, Eq. (70) becomes:

$$\mathbf{e}(k) - \mathbf{e}(k-1) + T_s\eta\mathbf{e}(k-1) = T_s\mathbf{\Delta}(\mathbf{x}_d(k-1), \mathbf{x}(k-1)), \tag{67}$$

where T_s equals the sampling time. It is well-known that in order to obtain the asymptotic stability, it must be $\eta < diag(2/T_s)$, but in this case parameter η does not influence the reduction of the error. In fact, we can write the following relation:

$$\mathbf{e}(k) = (\mathbf{I} - T_s\eta)\mathbf{e}(k-1) + T_s\mathbf{\Delta}(\mathbf{x}_d(k-1), \mathbf{x}(k-1)). \tag{68}$$

If the Backward Euler sampling approximation is considered, then Eq. (66) becomes:

$$\mathbf{e}(k) - \mathbf{e}(k-1) + T_s\eta\mathbf{e}(k) = T_s\mathbf{\Delta}(\mathbf{x}_d(k), \mathbf{x}(k)). \tag{69}$$

If a non-exact cancellation is considered, then:

$$\dot{\mathbf{e}}(t) + \eta\mathbf{e}(t) = \mathbf{\Delta}(\mathbf{x}_d(t), \mathbf{x}(t)), \tag{70}$$

where $\mathbf{\Delta}(\mathbf{x}_d(t), \mathbf{x}(t))$ represents the cancellation error which can be assumed to be limited because the model of Eq. (53) is a minimum phase one. and in case of no-exact cancellation through parameter η it is possible to control the error: the bigger parameter η is, the smaller the error becomes. In fact, we can write the following relation:

$$\mathbf{e}(k) = (\mathbf{I} + T_s\eta)^{-1}\mathbf{e}(k-1) + (\mathbf{I} + T_s\eta)^{-1}T_s\mathbf{\Delta}(\mathbf{x}_d(k-1), \mathbf{x}(k-1)). \tag{71}$$

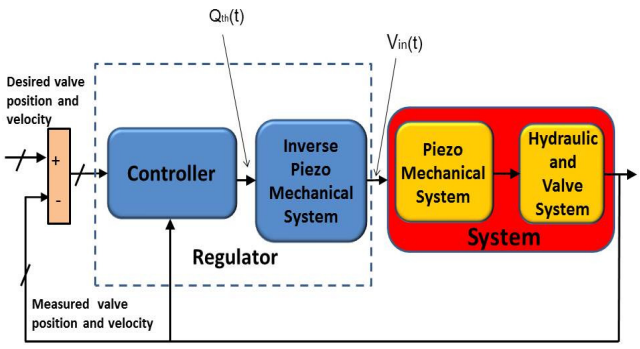

Fig. 6. Control scheme

5. SIMULATION RESULTS

The control scheme is shown in Fig. 6 in which the control law of equation (65) is visible together with the inversion of the piezo mechanical system. Figure 7 shows the final results concerning the tracking of a desired position of an exhaust valve with 8000 rpm. Figure 8 shows the final results concerning the tracking of a desired velocity of an exhaust valve with 8000 rpm. Figure 9 shows the desired and the servo piston position. The force acting directly on the valve at the opening time has a peak value equal to 700 N circa. This force is reduced to a few Newton acting on the piezo part thanks to the decoupling structure of the hybrid actuator. This is one of the greatest advantages of these hybrid actuators. The model of such kind of a disturbance is obtained as an exponent function of the position of the valve. The digital controller is set to work with a sampling time equal to 20×10^{-6} s, according to the specifications of the Digital Signal Processor which we intend to test the system with.

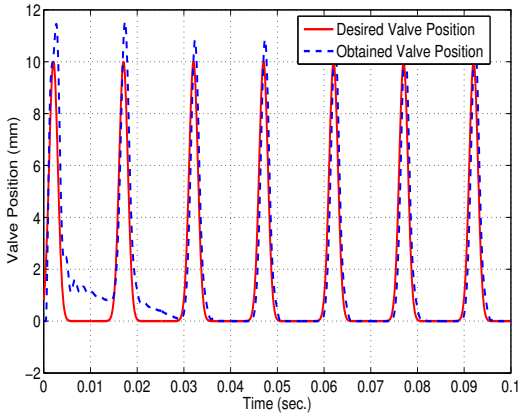

Fig. 7. Desired and obtained valve positions corresponding to 8000 rpm

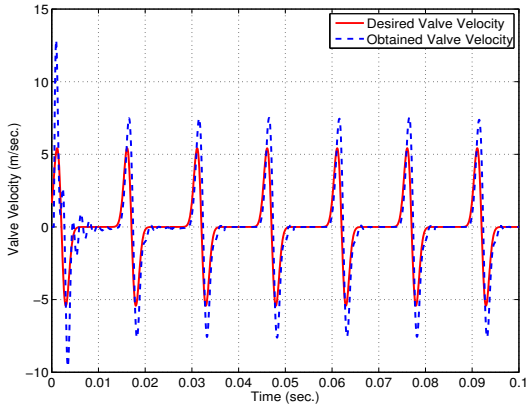

Fig. 8. Desired and obtained valve velocity considering 8000 rpm

6. CONCLUSIONS

This paper deals with a hybrid actuator composed by a piezo and a hydraulic part and its control structure

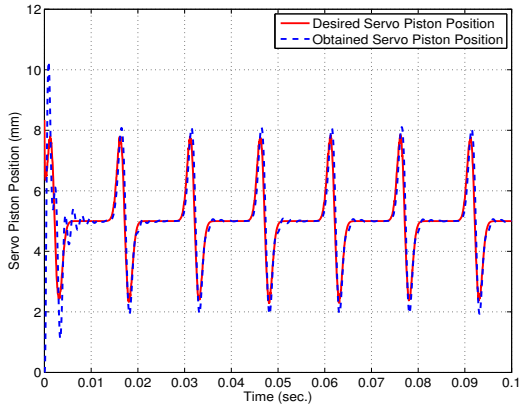

Fig. 9. Desired and obtained servo piston position considering 8000 rpm

for camless engine motor applications. The idea is to use the advantages of both, the high precision of the piezo and the force of the hydraulic part. The proposed control scheme considers a regulator which consists of an inversion of the piezo mechanical part and a Lyapunov based controller. Backward and Forward Euler sampling methods are compared. Simulations with real data of a motor and of a piezo actuator are shown for the controller realized by Backward Euler method.

REFERENCES

Adriaens, H., de Koning, W., and Banning, R. (2000). Modeling piezoelectric actuators. *IEEE/ASME Transactions on Mechatronics*, 5(4), 331–341.

Croft, D., Shed, G., and Devasia, S. (2001). Creep, hysteresis, and vibration compensation for piezoactuators: Atomic force microscopy application. *Transactions of the ASME Journal of Dynamic Systems, Measurement, and Control*, 123(1), 35–43.

Fabbrini, A., Garulli, A., and Mercorelli, P. (2012). A trajectory generation algorithm for optimal consumption in electromagnetic actuators. *IEEE Transactions on Control Systems Technology*, 20(4), 1025–1032.

Mercorelli, P. (2012a). An anti-saturating adaptive preaction and a slide surface to achieve soft landing control for electromagnetic actuators. *IEEE/ASME Transactions on Mechatronics*, 17(1), 76–85.

Mercorelli, P. (2012b). A hysteresis hybrid extended kalman filter as an observer for sensorless valve control in camless internal combustion engines. *IEEE Transactions on Industry Applications*, 48(6), 1940–1949.

Mercorelli, P. (2012c). A two-stage augmented extended kalman filter as an observer for sensorless valve control in camless internal combustion engines. *IEEE Transactions on Industrial Electronics*, 59(11), 4236–4247.

Murrenhoff, H. (2002). *Servohydraulik*. Shaker Verlag, Aachen.

Yu, Y.C. and Lee, M.K. (2005). A dynamic nonlinearity model for a piezo-actuated positioning system. In *Proceedings of the 2005 IEEE International Conference on Mechatronics, ICM* 10^{th}-12^{th} *July*. Taipei.